communications earth & environment | Article

A Nature Portfolio journal

https://doi.org/10.1038/s43247-026-03500-4

Climate change affects future sea-bed mobility via storms and sea level rise

Check for updates

Julia Rulent[1] ✉, Lucy Bricheno[1], Connor McCarron[2], Christopher A. Unsworth[3], Martin J. Austin[3], Richard J. S. Whitehouse[2], Nicholas G. Heavens[4,5], David P. Gold[4,6], Anthony Wise[1], Veerle A. I. Huvenne[7] & Katrien J. J. Van Landeghem[3]

How will climate change affect the composition of the seabed? Using three-dimensional hydrodynamic and wave models combined with climate projections from the Coupled Model Intercomparison Project phase 5, we investigate and quantify the drivers of seafloor stresses, using a North Western European Shelf case study. This study maps the potential for grain size mobilisation in present-day and future conditions, highlighting areas where transport capacity is likely to change. Sea level rise alters both absolute water depth and tidal dynamics, changing the magnitude and timing of seabed stresses while simultaneously reducing exposure to waves and currents. In contrast, increasing storm intensity in a warming climate is expected to cause more frequent episodic disturbance of an otherwise increasingly stable seabed. These predicted changes and their potential impacts on the benthic environment are discussed in the context of growing anthropogenic pressures and the associated challenges for marine spatial management.

The changing climate is having a rapid impact on the global ocean[1], particularly in coastal and shelf seas, yet few studies have investigated effects at the seabed[2,3]. To study this phenomenon, we focus on the regional area of the North Western European Shelf (NWES) as a case study; this region includes areas with diverse characteristics such as deep and shallow zones, varying tidal ranges, and differing waves and surge dynamics. These conditions can be found in other shelf seas globally. Though the quantitative estimates presented here reflect local processes, the underlying hydrodynamic processes are universal, and our findings are applicable to other regions. The direction of the response of seabed stress and currents to changes in sea level and storms is not a local issue. Sea level rise is occurring globally, and will affect shelf-seas worldwide. As such, other systems can draw insight from results obtained in this well-studied region, which is representative of a wide range of environmental conditions. Changing weather conditions (storm intensity and wind speeds), tides (amplitude and amphidrome position)[4–7], and sea level rise (SLR) will all act to alter the amount of energy reaching the seabed, but how will this change through time and across complex natural seascapes, and how will this impact shelf sediments and the habitats that rely on them? While SLR will act to decouple the wave base from the seabed, it will also allow more wave energy to transfer towards shorelines and the often densely populated coastal zones. Storms transfer energy to the seabed and increase sediment mobility (e.g.[8,9]). Any increase in storminess will grow wave height and period, thus increasing wave energy, and associated with the seabed exposure. The last two IPCC assessment reports[10–12] concluded that projections of future storminess remain uncertain. State of the art climate models (CMIP5, CMIP6) show a northward extension of the North Atlantic storm track, which could lead to increased frequency of windstorms over western Europe (e.g. ref. 13), with larger increases at higher global warming levels (e.g. ref. 14). Reference [15] predicts that UK storm severity could increase by around 30% by 2080, mainly due to storms covering larger areas. However, few studies focus on changes in storminess at mid-century[16] as large natural variability makes it difficult to detect clear trends in storminess. Deepening waters can change tidal asymmetries and, thus, regional sediment transport pathways. Even small changes in tidal regimes have the potential to change how anti-cyclonic tidal ellipses trap carbon on shelf seas[17–19]. An increase in annual average global temperature of at least 1.5 °C is now likely[12]. This warming will accelerate SLR and means we are certain to experience environmental change as a result; therefore, there is a pressing need to understand the impacts and plan for a changing seabed in our shelf seas.

Changes in seabed substratum and seabed morphology from alterations to seabed stresses can impact habitats[20–22] and the wider marine food webs[23,24]. The coarsening of seabed substrates is, for example likely to enhance species richness, abundance and productivity of the epibenthic megafauna[25]. Seabed stress acts as a key predictor of temperate reef habitats[26], and on sand banks, even subtle changes in the proportion of silt drive changes in important high-calorie epibenthic prey for deep-diving predators such as birds and marine mammals[27,28]. Seabed substrates in shelf

[1]Coastal Ocean, National Oceanography Centre, Liverpool, UK. [2]Coasts and Oceans, HR Wallingford, Wallingford, UK. [3]School of Ocean Sciences, Bangor University, Menai Bridge, UK. [4]Viridien, Crawley, UK. [5]Independent Researcher, London, UK. [6]Ecodetect Limited, Gaerwen, UK. [7]Seafloor Ecosystems, National Oceanography Centre, Southampton, UK. ✉e-mail: jrule@noc.ac.uk

seas, and the habitats that depend on them, are instrumental in the delivery of a variety of ecosystem services, including provisioning services (e.g. food, aggregates, genetic materials and biodiversity), regulating services (e.g. climate regulation, nutrient cycling and flood prevention) and cultural services (e.g. recreation such as diving or education)[29–32]. The need for detailed maps of seabed sediment types and seabed currents has been repeatedly flagged when investigating the suitability of sites for developing offshore renewable energy (e.g. windfarms), where accelerated development of infrastructure can occur to cut carbon dioxide emissions[33,34].

The interaction between flows and the rapidly growing amount of seabed infrastructure associated with, for example windfarms (turbines, foundations, cables and protective materials), may impact seabeds regionally, rather than just locally[35], and can make ecosystem-changing alterations[36,37]. Existing maps and model outputs of seabed stresses, mobility indicators and seabed sediments (e.g. refs. 19,38–42) are representative of historical or present-day conditions. To underpin marine spatial management that is future-proof, therefore able to withstand changes in storminess, seabed and the seabed environment, future changes from climate-related drivers need to be considered[43,44], and the impact on the bed stress from the infrastructure needs to be contextualised with the impact from accelerating climate drivers of change.

A recent poleward shift in North Atlantic storm tracks has been observed, together with an increase in storm intensity[45]. Retreating Arctic sea-ice will increase northerly fetch, wave height and wave period. These global changes will trigger regional impact and affect shallower regions exposed to northerly winds[46]. Based on our hypothesis, changes in surface wave height, fetch, period, and direction are thus expected to combine with SLR-modified seabed currents and alter seabed stresses, seabed mobility and the ecosystems that depend on it across all trophic levels. Changes like these from the accelerating climate crisis will occur globally, with localised impact over regions like the NWES used in this study; there is an urgent need to find a way to predict the consequences for energy transfer to the seabed and the consequences on wider ecosystems.

In this work, we use a 1.5 km resolution NEMO and WaveWatchIII model of the NWES to simulate seabed stresses and potential for seabed mobilisation. For the first time, the expected magnitude of future changes to seabed stresses and sediment transport capacity (i.e. the coarsest sediment the flow can mobilise, regardless of actual seabed composition) in space and in time is quantified from Representative Concentration Pathways (RCP8.5) mid- and end-century climate scenarios. This is a widely used high-emission scenario that, to our knowledge, has not yet been used for this type of study. To support long-term and more strategic marine spatial planning, we isolate physical controls on the seabed from sea level rise and storms to map the dominant drivers per region. Quantifying climate-driven impacts, assessed against present-day variability, this study examines how seabed stresses respond to the isolated effect of SLR, how future storm conditions under an extreme climate scenario may further modify seabed stress, and how the resulting changes in ocean currents and seabed stresses could influence future sediment transport capacity. We present a new, globally applicable method employed here in a NWES case study, as it has the opportune combination of being exposed to a wide variety of conditions (intense storms, large magnitude waves and tides[45]) and being one of the most industrialised shelf seas in the world[47,48]. This indicates that this region reflects a broad range of conditions present in other parts of the world and can provide insights for other rapidly developing shelf areas. Future seabed stresses and the potential for sediment mobilisation at the seafloor have never been assessed, neither in this region nor anywhere else in the world to our knowledge. Here we map a range of future seabed stresses driven by state-of-the-art predictions for future climate scenarios out to the middle and end of this century.

Results

Defining present-day natural variability

Any changes in bed stress brought about by climate change or seabed infrastructure must be put into the context of natural variability. In our case study area, as discussed in more detail below, large but predictable variability in seabed stress is generated over the 28-day lunar cycle. Regular tides can cause high seabed stresses in areas of high tidal range, such as estuaries and also where currents accelerate around headlands. The highest wave stresses are brought by large winter storms, and thus these stresses are only experienced periodically alongside calm periods of low wave stress. The largest wave stresses on the UK shelf are seen in shallow water, and also on Atlantic-facing coasts, which experience energetic long-period swells.

During the summer months, when there are few storms, the majority of seabed stresses are generated by tides. When the tides are dominant, the largest stresses are experienced in areas of fast tidal currents (straits and headlands) and in shallow water estuaries where the tidal range is large. For example at Anglesey, St David's Head, and Cherbourg, modelled current speeds reach 1.5 m s^{-1} on neap tides and can exceed 3 m s^{-1}on spring tides. These tidal currents correspond to seabed stresses of up to 4 N m^{-2} on neap and 8 N m^{-2} on spring tides. Comparing the monthly mean (Fig. 1c) and monthly maximum (Fig. 1d) stresses for June, the spatial distribution changes very little, as both the mean and maximum stresses in the summer are largely tidally generated. The range of these regular, predictable seabed stresses is generated by the spring-neap cycle.

During storms, wave-generated stresses can exceed tidally generated stresses. This can be seen by comparing maps of combined wave and current stresses during summer (June Fig. 1a) and winter (January Fig. 1b). The January mean (Fig. 1e) and maximum (Fig. 1f) conditions show rather different spatial patterns; the mean shows dominant stress signals over high tidal range areas, whereas the maximum (that can only be reached during storm times, i.e. strong waves) becomes enhanced over areas exposed to the Atlantic as well as over the shallow regions of the North Sea. While the monthly mean still has the same contribution of tidal stresses throughout the year, the monthly maximum shows how winter storms lead to strong seasonal increases in seabed stress. While the exact pattern of these wave-generated stresses will be dictated by the path of an individual storm track, there are some commonalities; storm-generated wave stresses are largest on Atlantic-facing west coasts, and in areas of shallow water. The modelled wave-generated seabed stresses can be of the order 1 N m^{-2} or less under average conditions, rising to over 10 N m^{-2} during storms.

To summarise, the average tidal stresses are around 5 times the size of average wave stresses, but under stormy conditions, a single storm can bring very large and short-lived disturbances at the seabed. In present-day winter, wave stresses under storm conditions can be more than 10 times larger than during calm conditions, generating stresses more than twice as large as the strongest spring tides.

Relative importance of storms and tide as drivers of seabed stresses

The stresses mapped in the section 'Defining present-day natural variability' are generated by a combination of wave and current processes. The UK continental shelf has distinct regions, and can be separated into near-coastal or shelf regions, which are dominated by either waves or tides. Figure 2c shows the fractional contribution to total seabed stress in January 2017 from waves and currents. Blue areas are controlled by waves, and brown areas are dominated by currents. Currents are seen to control the majority (up to 100%) of the stress in shallow coastal areas with fast tidal flow. Waves are the controlling process on Atlantic-facing coasts, and most of the North Sea. Beyond the continental shelf, seabed stresses are relatively weak and predominantly current-driven, as increasing water depth prevents surface waves from transmitting momentum to the seabed.

To summarise this spatial analysis of controls on seabed stress, the NWES domain is broken down into areas following the approach of ref. 49, specific to this shelf region. Figure 2a shows the regional decomposition. The same regions are used for analysis across both summer and winter. These regional summaries give a quick picture of seabed controls and help understand which areas will be most vulnerable to changes in storminess or tides. By compiling the regional contributions of each seabed-stress driver (i.e. tide and wave-derived stresses), we can rank and map their relative importance, visualising, to first order, which drivers should be considered

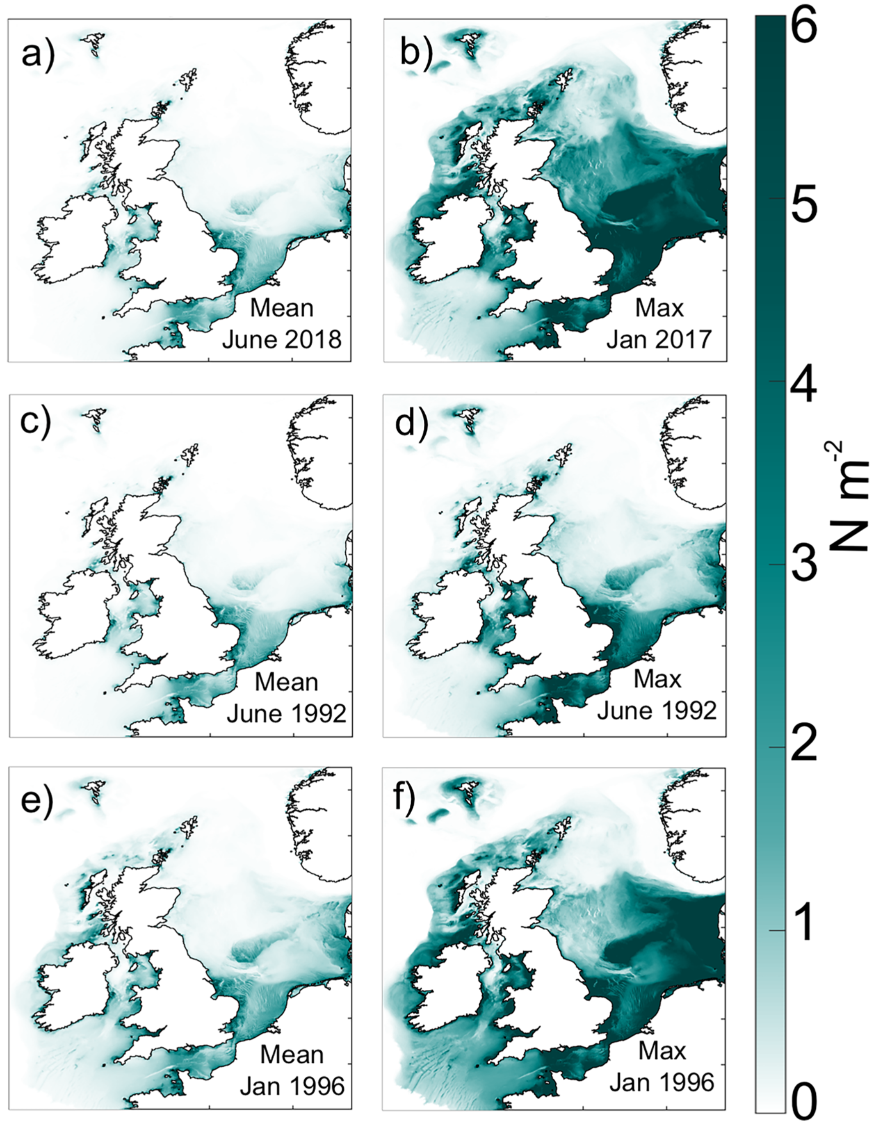

Fig. 1 | Combined seabed stresses for present-day runs. Monthly means (left) and monthly maxima (right). Hindcast runs summer mean 2018 (**a**) and winter maximum 2017 (**b**). HadGEM3-GC3 climate model forced runs for June 1992 (summer) mean (**c**), June 1992 maximum (**d**), and January 1996 (winter) mean (**e**) and January 1996 maximum (**f**). NB the colour scale is saturated at 6 N m^{-2} for visualisation purposes, though the maximum stress modelled reaches up to 8 N m^{-2}.

when estimating seabed stress. Bar charts in Fig. 2b, d show an integrated (spatially averaged) stress over each of the defined regions. The bar charts show the absolute contribution of waves and currents to the mean and maximum seabed stress. This allows us to visualise, per region, the relative importance of waves and currents in the summer vs. winter.

The range in magnitude of current-generated stresses is largely controlled by the spring-neap tidal cycle. For all regions, it varies little between summer and winter. Regionally averaged monthly mean current stresses are less than 2 N m^{-2}, with monthly maxima between 1 and 6 N m^{-2}. The wave stresses, however, are seen to change considerably with seasonality. Mean wave conditions in the summer are almost zero, with some small summer storms bringing an additional 1–2 N m^{-2}, whereas the winter mean and maximum wave contributions are more significant, exceeding 6 N m^{-2} in the North Sea. In parts of the North Sea, the regionally averaged winter wave component can be larger than the stresses generated under spring tides. Wave-dominated areas, as mapped in Fig. 2c, have the largest seasonal variation in total stresses.

Sea level rise impacts on seabed stresses

As rising sea levels will affect the propagation of the Kelvin wave that drives tides throughout the NWES, the two experiments described here explore how future SLR may shift the behaviour of this tidal wave, and the associated seabed stresses. To isolate this effect, we run a hindcast simulation for June 2018 twice; once with realistic present-day forcing, then with identical weather and open ocean conditions, but this time including SLR at the open boundary. The estimate of sea level added is spatially variable and derived from the work of ref. 50; the average SLR contribution to the boundary was an additional 0.28 and 0.70 m for mid- and end-century, respectively. This includes contributions from surface mass balance and ice dynamics of the Greenland and Antarctic ice sheets, as well as from land-based glaciers and land water storage (e.g. groundwater extraction or reservoir impoundment), but does not include ocean dynamic contributions[50].

Figure 3a, b shows projections of future mean and maximum summer stresses (compare with Fig. 1a, b, which include no SLR). Spatially, the patterns are largely similar, showing a smooth response, with no shocks in the system. There are both increases and decreases in tidal range and phase, with the largest changes associated with high tidal range in estuaries. SLR impacts the behaviour of the tides in a spatially varying way. In this experiment, the perturbed tidal range (Fig. 3c) is similar to present-day, but clear spatial changes are seen when taking a difference plot (Fig. 3d). The movement of the tide (location of amphidromes and tidal current's speed) is altered, as is the difference between water levels at low and high tide. This movement of amphidromes (points of zero tidal range) can increase or decrease tidal range at some sites. For example the Irish Sea sees increased range of up to 0.4 m, while a decrease of up to 0.5 m is seen in the Gulf of St Malo. The impact of SLR on the tide is amplified in estuaries, for example in

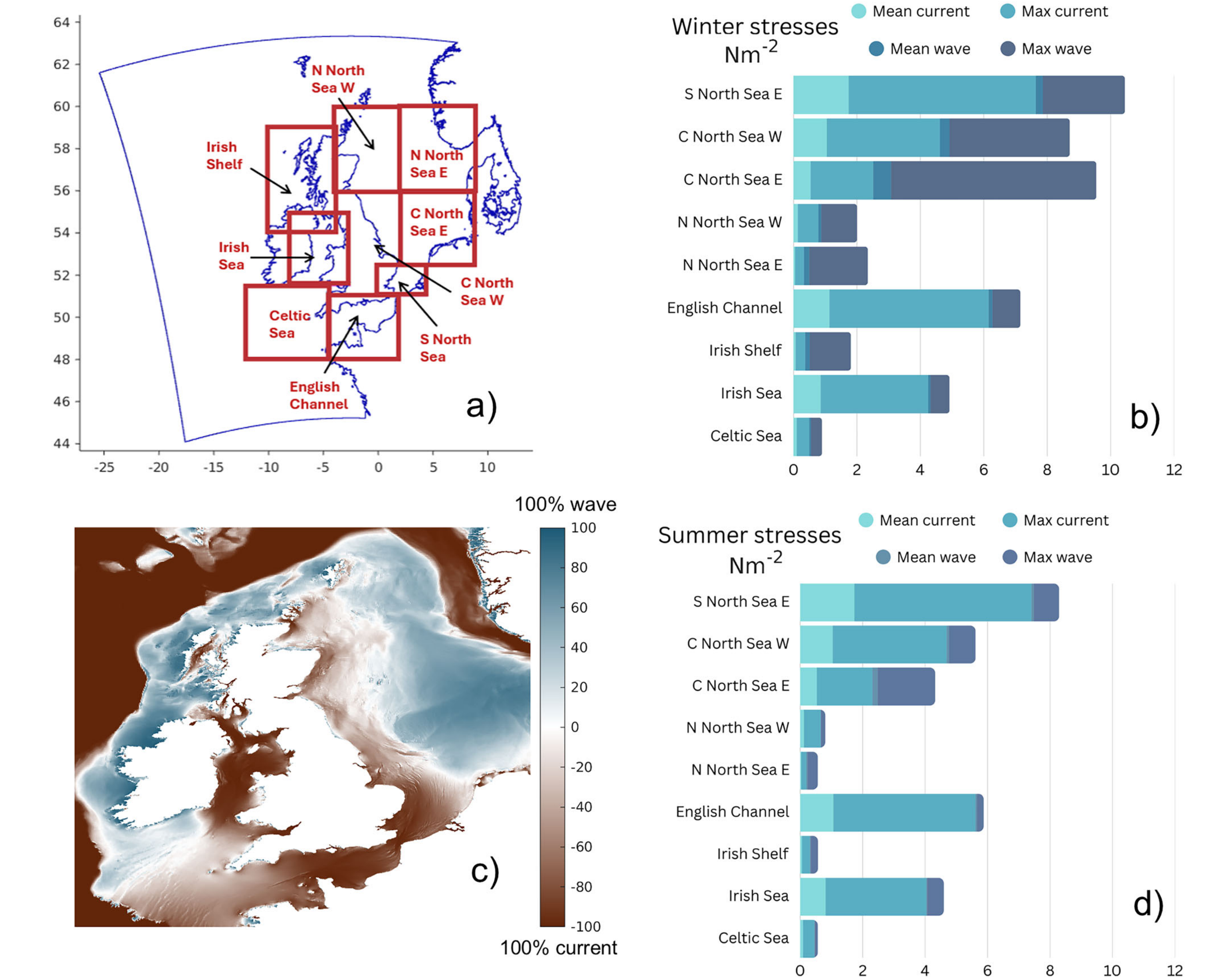

Fig. 2 | Regional analysis of contribution to the total seabed stress from waves and current. Map showing areas selected for regional analysis (**a**), regional dominance of wave vs. current stresses during January 2017 (**c**), bar charts illustrating the mean stress contribution (N m^{-2}) for each region defined in (**a**), for winter (**b**) and summer (**d**). Each bar is decomposed into its stress components to highlight seasonal changes in mean and maximum stress derived from the WaveWatchIII model wave and NEMO currents constituents.

Morecambe Bay and in the Solway Firth. Another intermediate experiment (not shown) was carried out for future projections of SLR in 2050; in this case, spatial patterns remained the same. The response of the tide to SLR was to increase the total water level by ±0.2 m with respect to present-day, compared with ±0.4 m by 2100. The projections in changing water levels are similar in pattern to those made by 2D models from refs. 4[5] and the 3D model of ref. 51, who also add sea level to present-day tide to ensure consistent astronomic forcing.

As well as impacting the tides, SLR simply increases total water depth. Tidal dissipation occurs when currents experience bottom friction at the seabed. SLR decouples surface currents from the seabed, as discussed by refs. 52–54. Briefly, the increased water depth reduces the direct influence of bottom friction on surface flows so that surface currents respond more strongly to wind forcing and pressure gradients. As a result, momentum transfer to the seabed is weakened, partially decoupling surface currents from benthic dynamics. The tidal dissipation decreases with increased SLR, as generally deeper water generates less stress on the seabed. Across the shelf, the maximum change caused by SLR is relatively small; of the order 0.3 N m^{-2} (Fig. 3e). There are some hot spots, where SLR has a more substantial influence on seabed stresses. Where tidal range is highest (e.g. in Morecambe Bay, the Mersey and Severn estuaries), the impact of SLR is seen more strongly. Much stronger reductions (of the order 1 N m^{-2}) are predicted in shallow waters. An exception to this is a reduction of 0.2 N m^{-2} at the Dogger Bank, but this site has low tidal range, being close to 2 amphidromes. There is a second-order effect of shifts in tidal current speed, caused by the changing positions of the amphidromes (Fig. 3c, d), which can move up to 3.8 km in our end-of-century experiment. These tidal changes can alter seabed currents by up to ±0.05m s^{-1}, changing stresses by up to ±0.01 N m^{-2}. However, these changes are modest, compared to the effect of deepening the water everywhere, which is the dominant process.

SLR can also alter the wave stress (Fig. 3f). Following the same mechanism as for currents, SLR acts to decouple the impacts of storms from the seabed and reduces the overall stresses felt during a passing storm[55]. This impact is seen more strongly in areas of shallow water (e.g. Dogger Bank). As total water depth increases, the sea-surface moves further away from the bed, and thus the wave energy cannot penetrate as deeply. The impact of SLR on wave stresses is small, less than 0.2 N m^{-2} at its maximum. The most energetic waves experienced by the UK are long-period swells moving across the Atlantic. The longest 'swell' waves are also more affected by the change in sea-level. Longer waves interact with the seabed in deeper water depths than

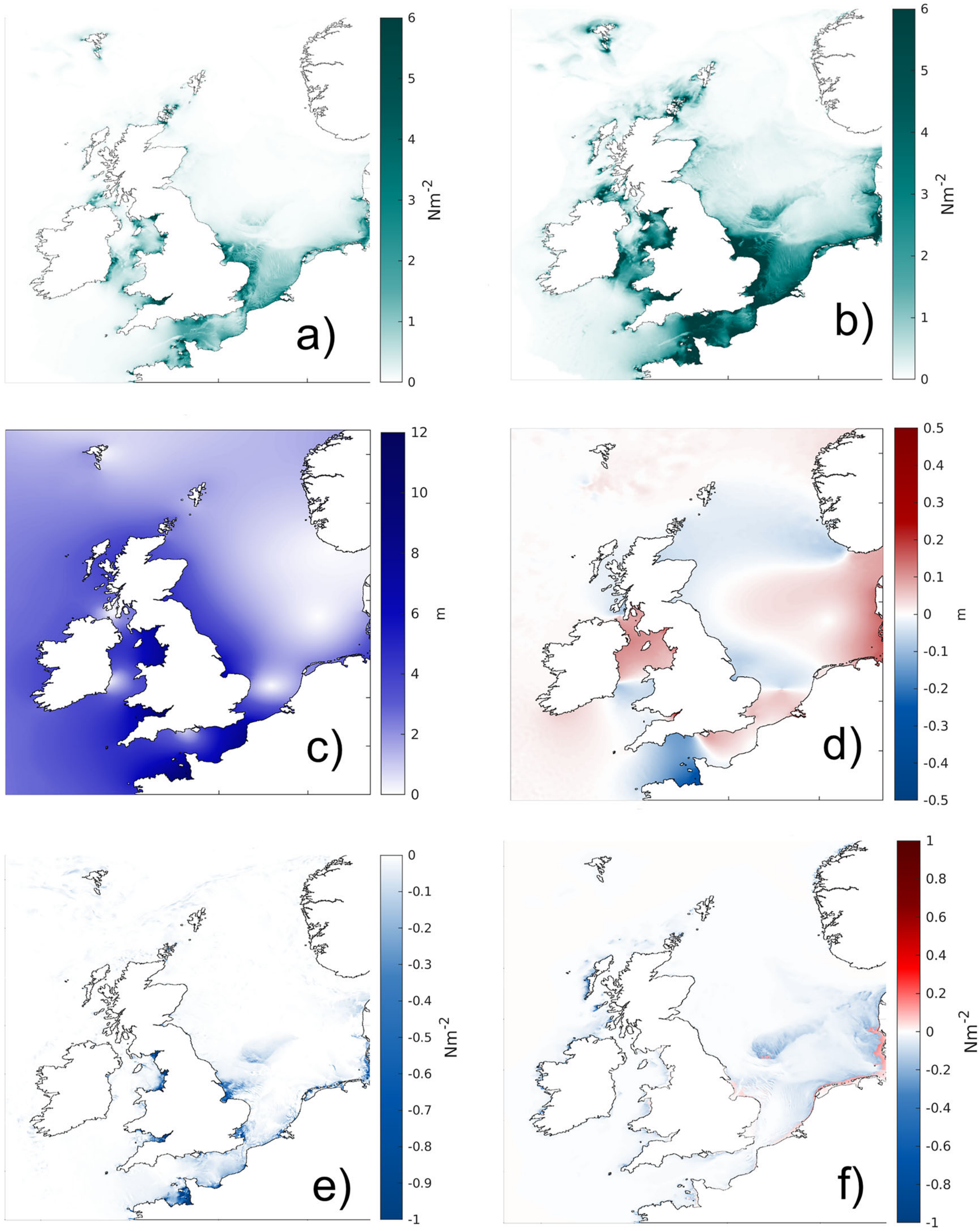

Fig. 3 | Impact of SLR on tidal behaviour and seabed stress. Subplots show the results of a sensitivity experiment aimed at isolating the effect of SLR, by adding increased water level at the model open boundary, while keeping all other forcing unchanged from June 2018. Monthly mean stress (**a**), and monthly maximum stress (**b**), the tidal range in the 2100 SLR experiment (**c**), and the difference between 2100 SLR experiment and present-day tidal range (**d**). The impact of SLR on the tidal component of stress is shown in (**e**), and the impact of 2100 SLR on wave stress in (**f**).

short waves, and dissipate more energy as they approach the coast. With the increased sea level, these swell waves cannot reach the seabed as easily, so the stresses on the seabed are reduced. With SLR, the wave stresses are reduced almost everywhere. In the spectral wave model, water depth alters dissipation by activating shallow-water loss mechanisms, consequently changing the bottom friction dissipation, as described in more detail in ref. 55. As this is a blanket effect, experienced across the shelf, the reduced drag on waves in deeper water is integrated, allowing more energy to propagate to the coast. This reduction in shear stress will reduce dissipation and allow the waves to reach the coastline, resulting in a potential increase in wave height and shear stresses at the coast. This effect can be seen in (for example) the German Bight, where both the maximum wave height and stresses are seen to increase in the SLR experiment. As northerly waves approaching this coast have not dissipated as much energy (for instance, when travelling across Dogger Bank) at the seabed on their approach, the incoming wave energy is therefore higher. This aspect of SLR is likely to increase coastal hazards from waves and requires further investigation with detailed local models.

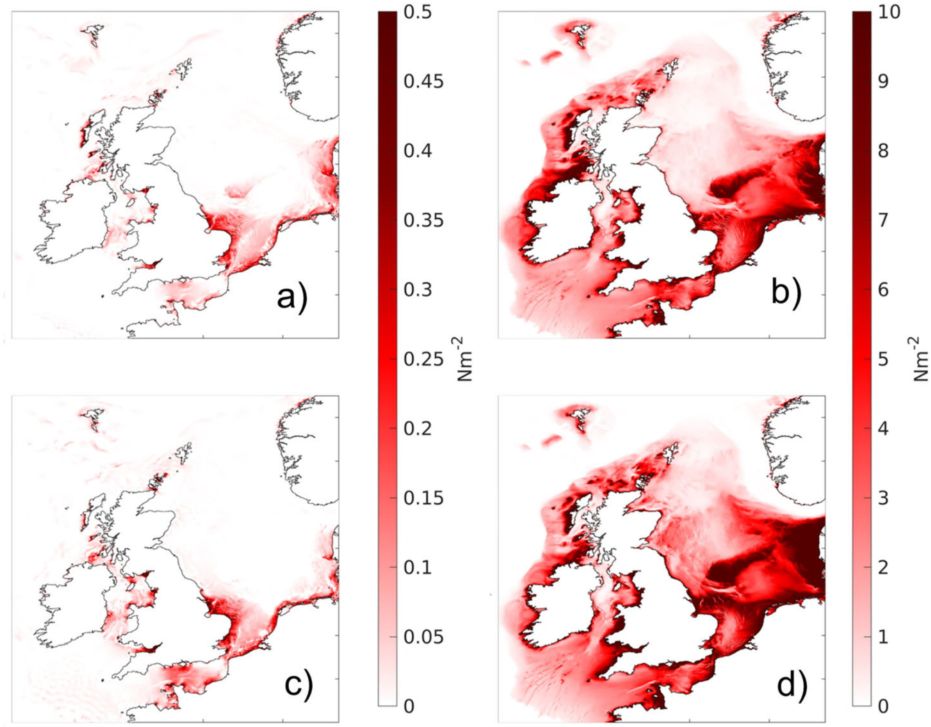

Fig. 4 | Impact of storminess on seabed stresses. Left-hand plots show the change in monthly mean stress (future minus present-day) in summers. Right-hand shows difference in monthly maximum winter minus summer for the same decade. Top row is mid century and bottom row is end century. June 2053 minus June 1992 (**a**), January 2050 minus June 2053 (**b**), June 2093 minus June 1992 (**c**), and January 2090 minus June 2093 (**d**). Note that we use a different range in the colorbar axis to better show summer and winter differences.

It is important to note that SLR is certain to continue in future, reducing both wave and current stresses at the seabed. SLR is the least uncertain facet of climate change as there is evidence that it will almost certainly keep rising at a rate that may accelerate[56–60], so while these changes are quite modest, our confidence assessments are high. However, there is less certainty with regard to the magnitude and speed of the sea level increase[56,61,62]. Similarly, there is limited confidence in projections of future storm intensity and frequency[63–66], making their impact on seabed stress uncertain, as it will depend on the characteristics of individual extreme events as we explore in the section 'Storms and sea level rise impacting future seabed stresses'.

Storms and sea level rise impacting future seabed stresses

Beyond SLR, the changing climate will also alter the frequency and magnitude of storms and extreme wave events[12,67]. Including predicted atmospheric changes into our analysis, such as varying winds and weather systems, together with SLR, permits an assessment of their combined future contributions to seabed stresses (see the section 'Simulating impacts from future climate change' for methodology). Figure 4 shows the impact of storms on wave-generated seabed stresses, demonstrating the maximum potential impact of future waves. In the summer (Fig. 4a, c), we predict a slight increase in mean future stresses, of the order $0.2-0.5\,\mathrm{N\,m^{-2}}$, with largest increases seen in the Southern North Sea and English Channel. These are representative of the background climate change signal that can be expected in quiet conditions[45].

The impact of winter storms has the potential to raise seabed stresses across the whole shelf by more than an order of magnitude. Comparing winter minus summer, we can see how the combined seabed stresses vary over the seasonal cycle in the future. Figure 4b, d shows the difference between summer and winter stresses in the middle and end of the century respectively. From summer to winter, increases in wave-generated stresses, in the order of an additional $8\,\mathrm{N\,m^{-2}}$ under a strong mid-century winter storm and $15\,\mathrm{N\,m^{-2}}$ under a strong end-century winter storm, are predicted (Fig. 4d). These impact the Atlantic-facing west coasts and shallow water regions most strongly, but almost all areas of the NWES see increased stresses of at least $1\,\mathrm{N\,m^{-2}}$.

To put this in context, future projections of storminess around the UK[45] indicate a stilling of waves in average (and summer) conditions, with an increase in winter storminess. This strong difference between winters and summers, will lead to more impactful bed disturbance, on more quiescent background conditions. This is an end-member experiment to see the maximum possible effect of future storm waves at the seabed. It is a single realisation of the most 'extreme' future month as predicted by this model, and shown as a bounding example of all possible futures; rather than a statistically robust estimation of 'typical' conditions. It shows that any climate change signal will be dwarfed by natural seasonal variability.

Future seabed stresses changing sediment transport capacity

Using the new bed shear stress maps we have generated (Fig. 5), it is possible to estimate the sediment transport capacity on shelf. Here, the seabed composition is considered non-cohesive and without biological components. This is a practical way of standardising the forces experienced by the seabed, while being agnostic of existing seabed type. A more complete estimate of seabed mobility would require shelf-wide measurements of the existing sediment grain size. However, this is primarily dependent on the quality and spatial coverage of the measurements of the grain size on the shelf. While shelf-wide maps do exist (for example ref. 39), they are of lower resolution than our numerical model (Supplementary Information in S1.3, Fig. S4). Therefore, we have instead inverted the problem; we calculate which maximum median grain sizes would be mobile for a given bed shear stress at every location on the shelf (Fig. 5). Using this approach, we quantify how typically calm summer months produce a lower mobilisation of sediment compared to the stormy winter months. For example in the present day, average wave stresses are typically of the order $2\,\mathrm{N\,m^{-2}}$, which can move sediment smaller than fine gravel (i.e. less than 2 mm). Storms can increase the combined seabed stress to above $10\,\mathrm{N\,m^{-2}}$, which can mobilise up to pebble-sized sediment (i.e. less than 11 mm), therefore increasing the range of sediment sizes which could be mobilised relative to average conditions.

Figure 5 shows maps of the median sediment grain size (often referred to as D50), which could be mobilised by modelled monthly maximum stresses. Figure 5a–f shows the monthly mobilised sediment, separated into Wentworth classifications[68]. There are clear seasonal differences in the areas

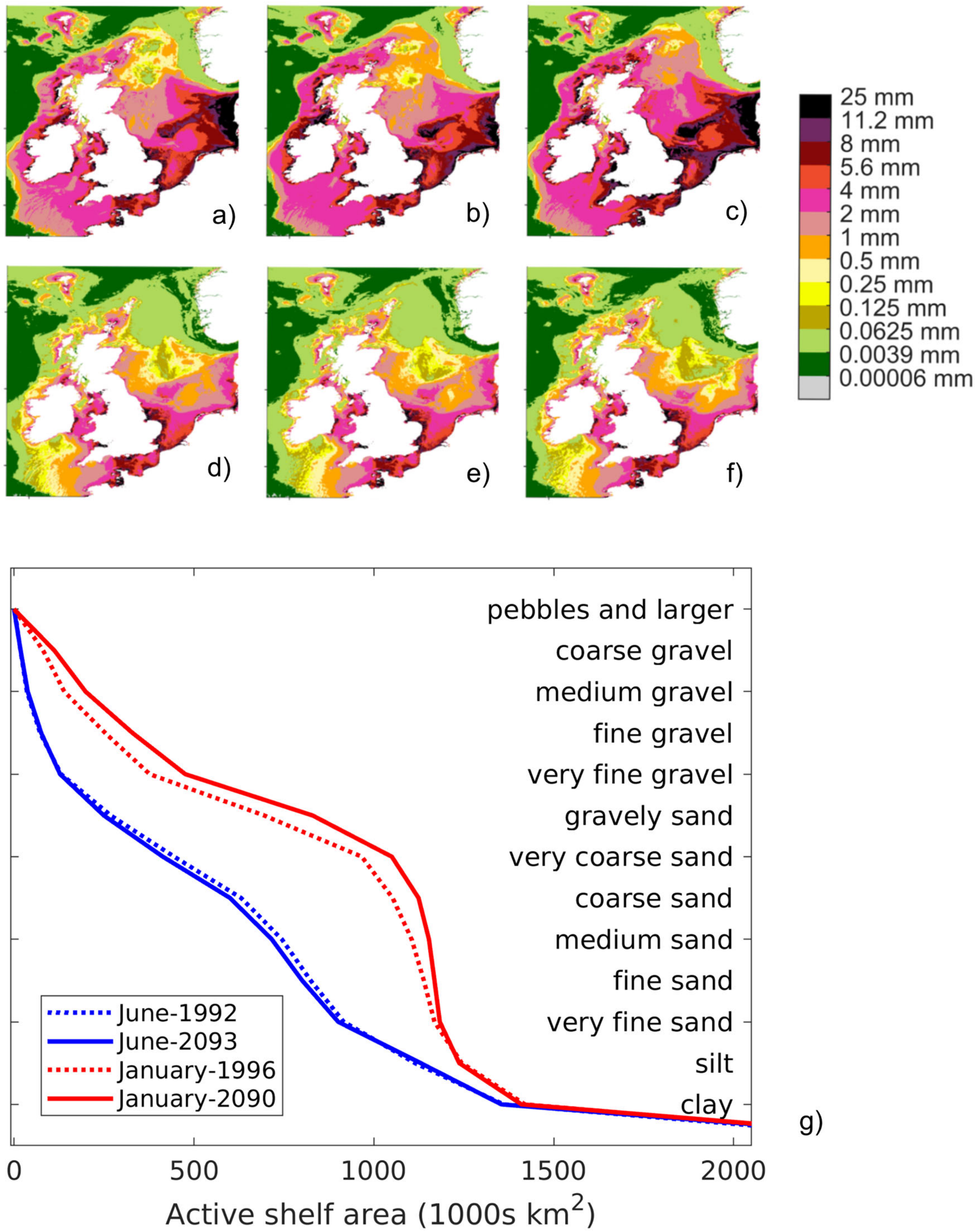

Fig. 5 | Seabed transport capacity under future scenarios. Median grain size mobilised by monthly maximum stresses of simulations including climate change forcing for January 1996 (**a**), January 2050 (**b**), January 2090 (**c**), June 1992 (**d**), June 2053 (**e**), June 2093 (**f**). The colorbars are divided into categories as defined by Wentworth[68]. Cumulative area (1000s of km^2) of shelf over which each sediment size class could be mobile for four different periods (**g**).

and grain sizes. In winter, large areas of the shelf experience stresses capable of moving gravels greater than 2 mm in diameter. In the summer, this drops to support only fine sands (between 0.0625 and 0.1 mm). Where tides are strong (e.g. in estuaries and English Channel), there is little difference between summer and winter, with combined stresses able to mobilise sediments of 11 mm or more. On Atlantic-facing coasts, large wave stresses can mobilise pebbles above 25 mm at the peak of the storms.

The seasonal and climate impacts can be explored further by summing up the active area of the whole shelf for each of the grain size classes. Figure 5g shows the cumulative area of shelf which is mobile for each grain size, comparing summers and winters in both present-day and end-century runs. During the winter, larger areas of the shelf experience stresses able to mobilise coarser sediments. The seasonality has the potential to change active sediment class over an area larger than 500,000 km^2 showing how storms are generating bed stresses capable of moving coarser sediments over a larger area. There is little difference in cumulative activity between historic and future summers, with a slight reduction shown in mobility of the sands. We also predict an increase in sediment mobility between past and future winters. In the end-century storm, we find that areas up to 100,000 km^2 have an increased capacity for movement in every class from fine sand and above when compared with the historic winter.

In all our future projections, tidal stresses on the shelf are expected to reduce with an overall reduction in seabed currents, as SLR deepens the water column, weakening momentum transfer between the surface and seabed. This is true for waves as well as tides (because wave orbital motions decay exponentially with depth). Conversely, there is amplification of wave-induced stress from storms, as events in this case study projection are more intense than those of the present-day storm simulation. In a warming world, higher sea surface temperatures fuel stronger storms towards the end of the century (e.g. ref. 15,66). This is represented by results (Fig. 5c). The increased strength of winter storms, combined with a reduction in stresses due to SLR, also increases the contrast between seasons in the future. By end-century, seasonality has the potential to change active sediment class over an area larger than 640,000 km^2 from summer to winter. West-facing coastlines and shallow sand banks are particularly susceptible to these climate-induced changes to sediment transport capability.

Whilst our projections are based on a single typical storm track for the area, each individual seabed disturbance event will have a spatially different footprint and unique magnitudes across the area. Our predicted values of sediment transport capacity are therefore not upper limits, but rather indicate a general direction of change of increased seabed mobility. By highlighting the range of possible changes in mobile grain size, these results help identify sensitive regions and magnitudes of potential seabed impacts.

Discussion

This study highlights the influence of SLR and storms on future seabed mobility, based on the projections of the RCP8.5 scenario. We focus on the NWES region, as it is a well-studied area, exhibiting a wide variety of conditions found across continental shelves globally, increasing the broader applicability of the results. Three main questions are addressed: How will the seabed stress be affected by the isolated effect of SLR? How will climate change (future storms) impact on future seabed stress in a case study extreme scenario? How can these projected changes in ocean currents and seabed stresses influence future sediment transport capacity? This study is purely modelling-based, and focuses on the effects of SLR and storms within a broader set of controlling factors which cannot all be considered here, such as mixed sediment classes and biological or compositional variability. Below, we first discuss direct implications of our results, followed by a broader speculative assessment of important concepts related to these findings. Limitations and future work are also discussed.

Results show that increased water level alone, when isolated from other climate change effects, will lead to an average reduction in seabed stress, reducing tidal bed current speeds and decoupling the waves from the seabed, diminishing wave-derived stress. These changes are on the order of 0.3 and 0.2 $N\,m^{-2}$ for tidal current-driven and wave-driven stresses, respectively, which is relatively small compared to seabed stresses driven by present-day spring tides (6 $N\,m^{-2}$) and storms, which can generate even higher stresses (up to 10 $N\,m^{-2}$). These natural wave and current stresses are smaller in magnitude than the anthropogenic stresses generated by seabed structures and fish trawling. For example infrastructures such as monopiles are known to influence seabed stress[69,70], potentially doubling the seabed drag coefficient in their wake and thereby increasing shear stress[70]. Another example is bottom-contact fishing, which is one of the strongest human disturbances to the seabed. Each pass of a bottom trawl can penetrate 1–10 cm into soft sediments[71]. The most impactful gear (beam trawls) can produce short-lived spikes of up to 20–40 $N\,m^{-2}$. The most widespread approach (using Otter trawls) can generate trawl-induced bed shear stress values of 1–10 $N\,m^{-2}$[72]. Overall, future changes to the seabed stress signal driven by SLR (and related tidal changes) are small in this context, but they are predictable and can be estimated for a range of future scenarios, as it was done here for RCP8.5. Conversely, based on this work, extreme storms are anticipated to increase seabed stresses and associated sediment mobilisation. There is a strong seasonal impact of seabed stresses mobilising sediment in the present-day. In future, we expect the strength of the seasonality to increase, widening the differences between winter and summer stresses. It was demonstrated that in this case study, seasonality can alter the active sediment class across an area exceeding 640,000 km^2 from summer to winter by end century. Where bed stresses are altered due to the effects of climate change, particularly in shallow regions, there will be an increased sensitivity of seabed sediment mobility, regardless of any potential seabed infrastructure development. Numerical simulations developed in this work reveal that storms can increase the seabed stress with up to an order of magnitude compared to average calm conditions, and this difference will increase in future. Individual storms are unpredictable (where and when they occur), but here we quantify the impact that an individual event can have, and how this is projected to change in the future. While a general stilling of the mean wave conditions is predicted in the context of global climate change, more frequent and more intense storms are predicted to cross North West Europe, bringing more energetic waves[45]. This study quantifies how and where increased sediment mobilisation may occur by the end of the century from such intensified storms (see Fig. 5). The combination of the general stilling and the increased stresses from transient events (storms) could exacerbate impacts on seabed habitats, as longer quiescent periods would be interrupted by more intense seabed disturbance during storms.

It is important to consider all these results within the context of the CMIP5 RCP8.5 projection, used here on a downscaled regional application[50,73], and the associated uncertainties. This work provides an understanding of seabed stress and transport capacity changes in an extreme scenario case, therefore it improves our understanding of the tail risk of a specific physical projection; these results do not show a statistical characterisation of future conditions. There is high confidence on the effect of tides, that in present-day simulations can contribute up to 3 $N\,m^{-2}$ to the total combined stress during spring tides in the NWES (tidal range of up to 12 m). There is less confidence in the effects of present-day storms, which, although generally well understood, involve short-timescale processes that remain complex to predict with high natural variability. In this work's simulation storms contribute up 12 $N\,m^{-2}$ to the total stress. When interpreting the projected results, there is high confidence within the scientific community that sea level will rise, with UKCP18 indicating an uncertainty range of 0.56–1.12 m[50]. This study shows that SLR can lead to a reduction of up to 1 $N\,m^{-2}$ in the total combined tide and wave-driven seabed stress under average conditions. However, there is low confidence on the state of future climate and storms, which we show are expected to contribute up to 15 $N\,m^{-2}$ to the seabed stress. Therefore, while SLR and associated background changes are expected to produce largely predictable, predominantly reduced seabed stresses, extreme storm events remain far less predictable and may continue to exert a dominant and potentially disruptive influence.

Beyond the direct results of this study, possible consequences and related concepts are considered, which remain uncertain but may be important for understanding the broader context, the significance of these findings, and guiding future research. Firstly, changes in sediment mobilisation can impact the development of offshore infrastructures[40,74,75]. The latter are developing quickly and worldwide in coastal and shelf regions, with aquaculture, platforms (oil and gas), as well as offshore wind farms, as some of the most frequently observed[76]. North West Europe and Asia (China in particular) are expected to show some of the largest increases in offshore infrastructures in the coming decades[77], largely in relation to the development of offshore wind farms[77]. The NWES region already supports operational offshore windfarms, with turbine arrays installed in increasingly deep waters[76,78,79]. This region will experience greater exposure to future storm events[16,45,66,80,81] and the associated enhanced seabed shear stress. Near offshore infrastructure, forces will be dominated by local flow amplification. In the far-field of infrastructure, however, the impacts on the seabed driven by the changing climate, as shown in this work, will interact and combine with the modified flows around the infrastructure, and this requires further investigation as it defines the future integrity of the seabed, its habitats and associated benthic biodiversity and ecosystem services[25,82]. Enhanced bed shear stress driven by climate change modifications to waves and tides will also change sediment mobility around offshore infrastructure. Enhanced seabed stresses can force a live-bed regime to transition to one that supports bedform development and migration[83] or drive change towards an upper-stage plane bed by flattening bedforms; seabed scour can result from both, exposing foundations and seabed cables to potential damage. These changes will also enhance the energetics of the turbulent wakes that form in the lee of seabed infrastructure such as offshore windfarm monopiles. At the scale of an offshore wind farm, the co-occurrence of enhanced stress resulting from climate change and the turbulent wakes from seabed infrastructure can combine. These enhanced stresses have the potential to increase seabed heterogeneity (the spatial variability of seabed morphology) and modify grain size mixtures[70]; all of which are critical for the functioning of the benthic ecosystems[84]. Sediment transport capabilities also impact the success of nature-inclusive designs of marine infrastructure. The rock grade chosen to keep infrastructure protected should not be mobilised in the next few decades, whilst modified mattresses (a different type of rock armouring used in OWF foundations[85]) to be nature-inclusive may not withstand intense currents[86]. Changes to sediment mobility can cause cage sinking, where protective cages used to contain restoration substrates (e.g. oyster shells or other habitat material) become partially buried due to sediment movement. This, in general, calls for improved reef and housing designs to ensure long-term restoration success[87]. Our results point towards hotspots of areas where future changes in seabed mobility will need to be taken into consideration.

Another important broader implication in the context of this study is the way in which seabed stress may modify benthic habitats, and how this can consequently affect the design and management of Marine Protected Areas (MPAs) or measures to compensate for potential habitat losses. SLR and storms can both have a significant impact on these areas, and previous studies indicate that adaptive measures represent an effective approach for enhancing their environmental resilience[88–91]. Sediment transport, which can be induced by both SLR and storms[92], also can have an impact over these areas[93]. Impacts of winnowing and sand wave migration will alter the habitat suitability for different benthic communities[94]. Benthic habitats are also sensitive to periodic extreme events. The passage of a storm can lead to a step-change in benthic habitats and infaunal communities[95]. In areas of high flows and bed stress, benthic communities are exposed, more robust and opportunistic, so they can withstand a large range of natural variability[96]. Increased storminess may create more and bigger disturbance regimes for benthic communities. A better understanding of future transport capacity, as the one presented in this work, can be helpful to identify regions more vulnerable to changes. However, it is not yet clear whether sediment mobilisation will be sufficient to really alter the seabed composition and therefore the habitats. Sediment transport capacity does not easily translate to sediment composition. Moreover, D50 sediment classes do not represent sediment heterogeneity, and the changes in sediment also need to be modelled together with all the other drivers for benthic community distribution (e.g. temperature, primary production) to estimate what the combined effects will be. If the storms are only rare events, then the disturbance may not be enough to alter the benthic habitat (sediment composition) over a longer time. In that case, they will mainly change (increase) the disturbance regime to which the current benthic communities are exposed, causing additional stress to the species present. The impact will also depend on the underlying sediment type and thickness. Increased shear stress might not immediately change the substratum type. If changes are regular and long-term, it might change the energy climate for benthic communities, and therefore cause changes in species presence/absence and community composition. These seabed composition results must therefore be evaluated together with other factors that determine species composition. For example rapid warming and marine heatwaves[97]. However, the outcomes of this work give indications of potential changes in seabed drivers and identify regions of the NWES that are exposed and need to be taken into account when carrying out future species distribution predictions.

This study has given a new understanding of future seabed mobilisation over the NWES and changes to the near-bed hydrodynamics. Further advancement could be achieved running a coupled NEMO-WaveWatchIII system, as opposed to combining the stresses offline. Live coupling would better capture the feedback interaction between wave and ocean components[98–101], as in this configuration we are missing the transfer of momentum between ocean and wave models. This is beneficial to accurately represent shallow waters and should be implemented in future work. Many of the largest impacts we observe are taking place in shallow water regions, where the hydrodynamic-wave coupling will be most impactful. In this pilot study, we ran the model uncoupled and combined stresses offline to simplify the methodology, reduce technical complexity, optimise computation time, and maintain applicability. Another area of future study would be to have the hydrodynamics coupled to a shelf-wide sediment transport model, to see dynamic evolution of the seabed. Future work should also aim to contextualise these individual storms in a longer climatology. Here, we focus on representative events to demonstrate how these processes can influence the background system changes. Running longer simulations, over decadal periods, would also be useful to provide longer time series, from which we could infer statistically robust predictions of future changes to wave and ocean currents derived stresses. Moreover, we have focused here on the widely used RCP8.5 projections; this could be further developed by considering high-end sea-level scenarios that target regional, unlikely but not impossible, extreme sea-level changes even more explicitly (e.g. ref. 102). SLR will tend to decouple from the seabed. This is another area which has scope for follow-on work. For example the wave energy dissipation is reduced, allowing more wave energy to reach coastal regions in some areas, resulting in a slight increase in seabed stress as demonstrated in this study for the German Bight. This is an unexplored area which could stimulate future work and may benefit from a coupled wave and hydrodynamic model.

Part of the future work outlined above is already underway as part of the ECOWind ACCELERATE project (https://ecowind.uk/projects/ecowind-accelerate/), as for example the inclusion of OWF infrastructure on top of the climate change impact discussed in this paper, or the effect of changes over benthic ecosystem and seafloor habitat.

Conclusion

In this study, we investigated the impact that changes to future climate can have on the seabed. Having categorised areas of the seabed which are most exposed to waves and/or currents, we identified areas where seasonality and storminess are important. We quantified the magnitude of seabed stresses which are generated by spring and neap tides, and calm and stormy conditions. Next, this analysis was performed for future scenarios of SLR and climate change (combining storms and SLR), to identify the areas of seabed which are most likely to change in future. Our results show that SLR will impact on ocean currents near the seafloor and will alter the seabed stresses. The impact of SLR alone (including impacts on tidal range and phase) leads to small but highly predictable changes which will be consistent over time. SLR also causes waves to decouple from the seabed (relative to the present-day), leading to an overall reduction in seabed stress and energy dissipation. While the SLR brings a small but predictable and consistent change, future storminess is expected to bring rare but large seabed stresses. The increased difference between summer and winter stresses strengthens the seasonality, and therefore impact of episodic storm events. These storms will be able to locally increase the seabed stress by up to an order of magnitude in some regions. These larger events have the potential to outweigh the impact of the small (but regular) baseline change, and need to be understood and considered when planning operational structures. While individual storms can not be predicted years ahead of time, the potential impact of an extreme storm can be calculated to account for worst-case scenarios. The expected changes to the seabed stress have the potential to alter seabed mobility, and the benthic communities which rely on them. Experiencing a stilling of the seabed due to reduction in summer waves, and SLR, we expect longer quiescent periods. But an increased number and strength of winter storms, will lead to larger areas of seabed, and coarser sediments becoming mobilised. These altered sediment dynamics may impact on the benthic habitats, and the suitability of the seabed for offshore infrastructure.

Table 1 | Average estimate of SLR at the boundary of the full climate forcing under RCP8.5 scenarios (see the section 'Simulating impacts from future climate change')

Scenario	Year	Season	SLR (m)	Referred in text as
Jun-low	1992	June	0.00	present-day
Jan-low	1996	January	0.00	present-day
Jun-mid	2053	June	0.14	mid-century
Jan-mid	2050	January	0.19	mid-century
Jun-end	2093	June	0.25	end-century
Jan-end	2090	January	0.32	end-century

Values shown here are used as indicative estimates derived from the average difference between 1990's runs and the future projections; in practice, the sea level footprint is spatially variable.

Methods

Numerical model setup

The models used are described in the sections 'Hydrodynamic NEMO model; AMM15 configuration' and 'WaveWatchIII spectral wave model; AMM15 configuration'. The model forcing used for each experiment is specified in the sections 'Isolating the impact from sea level rise' and 'Simulating impacts from future climate change'. The underpinning hydrodynamic and wave models have been tuned and run in this AMM15 configuration, with previous calibration and validation studies published by refs. 99,100,103,104. In all experiments, an ocean model and a wave model are run in standalone mode (i.e. uncoupled). The seabed stresses derived from both models are combined offline to estimate the joint contribution to the seabed stress. The validation of our model outputs is provided in the Supplementary Information Section S1. For readability, we may refer to the different experiment periods as 'present-day', 'mid-century', and 'end-century' in the text. Below is a table summarising the details of each experiment (Table 1):

Hydrodynamic NEMO model; AMM15 configuration. The ocean model used in this work is the Nucleus for European Modelling of the Ocean (NEMO; ref. 105). The configuration used is the Atlantic Margin Model (AMM15; ref. 106), and is based on the publicly available revision of AMM15_C09_p2[107], with additions to read 360-day calendar boundaries and changes to the seabed stress diagnostic that are described below. This configuration features a domain with 1.5 km horizontal resolution and 51 vertical levels using a terrain-following coordinate system.

For efficiency, the AMM15 configuration uses a split-explicit time-stepping algorithm that separates the computation of the depth-mean velocity trends from the 'baroclinic' velocity trends, where the latter uses a longer timestep. In this case, the computation of bed stress is separated into two components: one associated with the depth-average current and another associated with the depth-dependent current. For stability, the AMM15 configuration also uses an implicit bed stress scheme, which means that bottom friction is calculated together with other processes using the velocity at the current timestep via a matrix inversion. The standard diagnostics in NEMO are not set up to output an accurate bed stress when the split-explicit and implicit schemes are used together. We have therefore modified the source code to account for these model configuration choices and thus enable us to output the bed stress. Note that changes are only made to diagnostic outputs; the underlying physical equations used by NEMO are unchanged.

WaveWatchIII spectral wave model; AMM15 configuration. The wave model used is the WaveWatchIII spectral wave model[108], version 7.12 created as part of the UK Met Office development's efforts. The domain covers the same area as the ocean model (i.e. NWES), with the same rotated 1.5 km resolution over shelf region. Model bathymetry is rounded to the nearest integer number of metres to the water depth of the NEMO model. This configuration of WaveWatchIII is forced by lateral boundary conditions updated hourly from a single-level SMC global wave with resolution ~50 km (run in-house). The reanalysis atmospheric forcing is given by the ECMWF ERA-5 Numerical Weather Prediction reanalysis[109]. Future projections are forced by HadGEM3-GC3 in both the regional and global wave models. The wave model has a spectral resolution of 10 degrees (36 directions) and 30 frequencies, with a high frequency cut-off at 0.04118 s. For the HadGEM3-GC3 climate model, the Gregorian calendar was switched to ingest forcing with a 360-day calendar (30 days per month). There is no sea-ice in the regional model, but the global model updated sea-ice maps daily.

Calculating the seabed stress

In this study, the bed shear stress at the seabed is calculated offline, as part of the model outputs post-processing. It is obtained by combining the current-generated shear stress estimated from NEMO with the wave stress derived from the WaveWatchIII bottom orbital velocities.

Current bed shear stress (τ_c) is estimated as per[110], as a function of the water density (ρ), barotropic current velocity in the model's bottom level (U_{bar}), and the drag coefficient (C_d) defined in the NEMO model based on roughness length (z_0) and the Von Karman constant (κ), with (e_{3b}) defining the model cell thickness[111]:

$$\tau_c = \rho C_d {U_{bar}}^2 \quad (1)$$

$$C_d = \left(\frac{\kappa}{\log(0.5e_{3b}/z_0)}\right)^2 \quad (2)$$

Wave-induced bed stress (τ_w) is estimated through the wave orbital velocity (U_w) as a function of the near-bottom root mean square velocity (U_{rms}), as per refs. 38,110. The friction factor (f_w) based on the roughness length (z_0), is derived in WaveWatchIII using a static look-up table[112], which is itself based on field and laboratory experiments reported by refs. 113,114.

$$\tau_w = \frac{\rho f_w U_w^2}{2} \quad (3)$$

$$U_w = \sqrt{2}U_{\mathrm{rms}} \quad (4)$$

Total combined bed stress (τ_{combo}) values are estimated from combined currents and wave bottom orbital velocities, and the angle between current direction and wave travel direction (Φ) as per ref. 110:

$$\tau_{\mathrm{combo}} = \sqrt{\left(\tau_m + \tau_w|\cos\Phi|\right)^2 + \left(\tau_w|\sin\Phi|\right)^2} \quad (5)$$

where

$$\tau_m = \tau_c\left\{1 + 1.2\left(\frac{\tau_w}{\tau_c + \tau_w}\right)^{3.2}\right\} \quad (6)$$

We take hourly wave stress from WaveWatchIII and hourly current stress from NEMO to calculate a monthly mean and monthly maximum τ_{combo}.

Present-day experiments

A present-day simulation covers the January/February 2017 and May/June 2018 periods. It is initiated from the operational configuration of AMM15 run at the UK Met Office. The ocean lateral boundary from Atlantic and Baltic is also provided by the Met Office; these are the previously-operational Met Office forcing products, based on the NATL12 model[115]. The ocean surface forcing data are from the ERA5 re-analysis[109]. The files are re-gridded to be used as forcing for the wave model over the same period. The wave model is nested within a global configuration of WaveWatchIII, run at 0.5° spatial resolution. Spectral wave data from this model are used to force the later open boundaries of the AMM15 wave model at hourly intervals. This present-day simulation represents real weather conditions and the water levels, mean currents, directions and bed shear stresses have been validated against observation, see Supplementary Information Section S1.

Isolating the impact from sea level rise

In order to isolate the impact of SLR alone from the more complex climate change signal, we run a set of experiments where estimates for mid-century and end-century SLR are added onto a present-day simulation without including any additional climate change impacts to the system. By adding SLR estimates to the boundaries and restart conditions of the model, without including projections of the atmospheric forcing (i.e. impact of storm and winds changes), we quantify the influence of the rising sea levels alone in idealised experiments, before moving onto a more complex picture.

The spatially varying values of SLR, which were imposed on the present-day simulation, were estimated from maps of total relative sea level change based on the RCP8.5 scenario, as per the storyline of ref. 50. SLR projections for mid-century (2050) and end-century (2100) periods were added to the ocean model water level at the boundary. The NEMO model bathymetry and coastline are held constant at the present-day level throughout all simulations. For the wave-alone future SLR experiments, an additional 1 m was added to all water depths to simulate a homogeneous rise. This is due to a restriction on precision in the wave model bathymetry. The seabed stresses from these two simulations (present day and forced with SLR), estimated as described in 'Calculating the seabed stress', are then compared. Moreover, a harmonic analysis of the ocean model's sea surface height outputs allows to investigate the impact of SLR changes on the tide's (M2 and S2 components) phase and amplitude.

Simulating impacts from future climate change

To broaden the scope of the research beyond the impact of SLR alone, we run a different set of experiments forcing the models with climate forcing projections, also under the RCP8.5 scenario's assumptions[73]. As well as including the SLR impact, this accounts for projected changes to ocean dynamics, atmospheric temperatures, winds, and related low-pressure systems that are expected in future under extreme, yet possible, conditions.

The simulation periods are selected from a HadGEM3-GC3 climate projection dataset[50]. The projection of wind data at Constable Bank (in the Eastern Irish Sea) is extracted from 1980 to 2100. The Eastern Irish Sea is close to the centre of our NWES model domain, and thus captures the majority of the storm tracks crossing this region.

The mean wind speed is estimated for each decade, and the monthly mean that deviates the least from the overall average is considered as a 'typical' period within that decade. This way we select a baseline near present-day, mid-century and end-century calm periods to investigate, respectively, June 1992, 2053 and 2093. To select extreme (i.e. stormy) periods, we rank the 90th, 95th and 99th wind speeds to select the month with windiest weather within the decade. We select January 1996, 2050, and 2090 as extreme winter periods.

The WaveWatchIII model is initiated from rest, and permitted a 1-month spin-up period, before each experimental run. The NEMO model is initiated from a downscaled AMM7 projection run[73]. The coarser (7 km grid) AMM7 dataset is interpolated over the AMM15 (1.5 km) grid. The northwestern area of our domain is not covered by the coarser dataset; however, a set of AMM15 boundaries consistent with these simulations was provided by the Met Office[73]; this data is not publicly available. By combining the AMM15 boundaries with the consistent, downscaled AMM7 dataset, it was possible to interpolate data over the missing region to create suitable initial conditions for the model. The method was validated by running a short case study that could be compared against overlapping 20 years simulation forced with the same set of boundaries. We developed this method to be able to run short simulations without a long spin-up time and include our modifications to the shear stress code. The same set of AMM15 boundary files were used to force the ocean boundaries in the simulation. The surface forcing was also preprocessed by the Met Office from a set of HadGEM3-GC3 simulations[73] under the RCP8.5 projections; this dataset is also not publicly available, but access can be granted by the Met Office. Each simulation lasted 2 months, one of spin-up time, the second month (Junes and Januaries) being considered for the analysis. The seabed stresses are then estimated as per the section 'Calculating the seabed stress'. To explore the spatial variation and relative dominance of wave vs. current stresses, we decompose our results into spatial regions. In this way, we can visualise the relative importance of driving factors and map the total stress from ocean currents or waves over the shelf regions.

To quantify the implications of these changes for sediment transport capacity, we calculate the coarsest sediment type that can be moved by the modelled seabed stresses. Seabed stress has the potential to mobilise or resuspend sediments. Different classes of sediment will have different thresholds of motion, beyond which they can be moved by the stress acting on the seafloor. The models used assume a homogeneous bed type and associated bottom drag. The value of the roughness length (z_0) used in the hydrodynamic model (3×10^{-3} m) corresponds to a median sediment diameter D50 of 36 mm, which would be categorised as pebble-sized. However, at our model scale (1.5 km), the z_0 must represent a 'form drag' associated to seabed features such as ripples and dunes, opposed to simply the grain size alone. Even with this simplified picture of homogeneous roughness, we can combine the modelled stresses with observed mapped sediment type D50 to improve our picture of potential seabed mobility. For each grain size, a critical shear stress (τ_{cr}) can be derived from the non-dimensional critical Shields parameter (θ_{cr}) to determine where sufficient stress is generated to move the sediment. The critical Shields parameter is calculated using the empirical solution of ref. 116. If the bed stress (τ_{combo}) is larger than this value (τ_{cr}), then the seabed will mobilise. (θ_{cr}) is defined as:

$$\theta_{cr} = \frac{\tau_{cr}}{(\rho_s - \rho)gd} \tag{7}$$

Where ρ_s is the density of the sediment, ρ is the density of the fluid, g is the acceleration due to gravity, and d is the particle size.

Please note that further details on the validation of this method for estimating D50 from the modelled seabed stress are provided in the Supplementary Information Section S1.3. Also note that complete outputs from our simulations are publicly available on CEDA archives; we share the main physical variables from the ocean model components[117], as well as the main parameters output by the wave model[118], and summary data on our seabed mobilisation analysis[119].

Data availability

The outputs of the regional-scale numerical modelling projection simulation supporting these findings of this study are publicly available on CEDA archives; we share the main physical variables from the ocean model components https://doi.org/10.5285/38626589-5885-fff9-e063-7086abc09721[117], as well as the main parameters output from the wave model https://doi.org/10.5285/38624d82-baec-fcd8-e063-7086abc0e25c[118], and summary data on our seabed mobilisation analysis https://www.bodc.ac.uk/data/published_data_library/catalogue/10.5285/3bc6687c-00ad-d305-e063-7086abc08650/[119].

Received: 5 September 2025; Accepted: 31 March 2026;
Published online: 16 April 2026

References

1. Holt, J. et al. Future climate projections in the global coastal ocean. *Prog. Oceanogr.* **235**, 103497 (2025).
2. Li, F., Dyt, C., Griffiths, C. & McInnes, K. L. Predicting seabed change as a function of climate change over the next 50 yr in the Australian southeast. *Geol. Soc. Am. Spec. Pap.* **426**, 43–64 (2007).

3. Weinert, M. et al. Modelling climate change effects on benthos: distributional shifts in the North Sea from 2001 to 2099. *Estuar, Coast. Shelf Sci.* **175**, 157–168 (2016).
4. Pelling, H. E., Green, J. A. M. & Ward, S. L. Modelling tides and sea-level rise: To flood or not to flood. *Ocean Model.* **63**, 21–29 (2013).
5. Pickering, M. D., Wells, N. C., Horsburgh, K. J. & Green, J. A. M. The impact of future sea-level rise on the European shelf tides. *Cont. Shelf Res.* **35**, 1–15 (2012).
6. De Dominicis, M., Wolf, J., Jevrejeva, S., Zheng, P. & Hu, Z. Future interactions between sea level rise, tides, and storm surges in the world's largest urban area. *Geophys. Res. Lett.* **47**, e2020GL087002 (2020).
7. Opel, L. et al. Three drivers of 21st-century changes in ocean tides. *J. Geophys. Res.: Oceans* **131**, e2025JC022719 (2026).
8. Hequette, A. & Hill, P. R. Response of the seabed to storm-generated combined flows on a sandy Arctic shoreface, Canadian Beaufort Sea. *J. Sediment. Res.* **65**, 461–471 (1995).
9. Clukey, E. C., Templeton III, J. S., Lane, B. & Akhtar, M. W. Wave-seabed observations and a combined approach to determine required burial depth of offshore power cables under large storm waves and currents. *Ocean Eng.* **285**, 115356 (2023).
10. Christensen, J. H. et al. Climate phenomena and their relevance for future regional climate change. in *Climate Change 2013: The Physical Science Basis. Contribution of Working Group I to the Fifth Assessment Report of the Intergovernmental Panel on Climate Change* (eds Stocker, T. F. et al.) Ch. 14, 1217–1308. https://www.ipcc.ch/site/assets/uploads/2018/02/WG1AR5_Chapter14_FINAL.pdf (Cambridge University Press, 2013).
11. IPCC. Summary for policymakers. in *Climate Change 2013: The Physical Science Basis. Contribution of Working Group I to the Fifth Assessment Report of the Intergovernmental Panel on Climate Change* (eds Stocker, T. F. et al.) https://www.ipcc.ch/report/ar5/wg1/ (Cambridge University Press, 2013).
12. Seneviratne, S. I. et al. Weather and climate extreme events in a changing climate. in *Climate Change 2021: The Physical Science Basis. Contribution of Working Group I to the Sixth Assessment Report of the Intergovernmental Panel on Climate Change* (eds Masson-Delmotte, V. et al.) 1513–1766 (Cambridge University Press, 2021).
13. Harvey, B. J., Cook, P., Shaffrey, L. C. & Schiemann, R. The response of the northern hemisphere storm tracks and jet streams to climate change in the CMIP3, CMIP5, and CMIP6 climate models. *J. Geophys. Res. Atmos.* **125**, e2020JD032701 (2020).
14. Feser, F. et al. Storminess over the North Atlantic and northwestern Europe—a review. *Q. J. R. Meteorol. Soc.* **141**, 350–382 (2015).
15. Priestley, M. D. et al. Forced trends and internal variability in climate change projections of extreme European windstorm frequency and severity. *Q. J. R. Meteorol. Soc.* **150**, 4933–4950 (2024).
16. Little, A. S., Priestley, M. D. & Catto, J. L. Future increased risk from extratropical windstorms in northern Europe. *Nat. Commun.* **14**, 4434 (2023).
17. Ward, S. L., Neill, S. P., Van Landeghem, K. J. J. & Scourse, J. D. Classifying seabed sediment type using simulated tidal-induced bed shear stress. *Mar. Geol.* **367**, 94–104 (2015).
18. Williams, M., Amoudry, L., Brown, J. & Thompson, C. Fine particle retention and deposition in regions of cyclonic tidal current rotation. *Mar. Geol.* **410**, 122–134 (2019).
19. Ward, S. et al. The role of long-term hydrodynamic evolution in the accumulation and preservation of organic carbon-rich shelf sea deposits. *J. Geophys. Res. Oceans* **130**, e2024JC022092 (2025).
20. Froján, C. R. B., Bolam, S. G., Eggleton, J. D. & Mason, C. Large-scale faunal characterisation of marine benthic sedimentary habitats around the UK. *J. Sea Res.* **69**, 53–65 (2012).
21. Damveld, J. H. et al. Video transects reveal that tidal sand waves affect the spatial distribution of benthic organisms and sand ripples. *Geophys. Res. Lett.* **45**, 11–837 (2018).
22. Thomas, S., Bartl, I. & Thrush, S. Climate change stress causes simplification of a benthic ecosystem network. *Estuar. Coast. Shelf Sci.* **324**, 109442 (2025).
23. Maravelias, C. D., Reid, D. G. & Swartzman, G. Seabed substrate, water depth and zooplankton as determinants of the prespawning spatial aggregation of north atlantic herring. *Mar. Ecol. Prog. Ser.* **195**, 249–259 (2000).
24. Henriksen, O. et al. Effects of sediment type and light availability on the burying behaviour of small sandeel (Ammodytes tobianus). *J. Exp. Mar. Biol. Ecol.* **577**, 152020 (2024).
25. Benoist, N. M. et al. Monitoring mosaic biotopes in a marine conservation zone by autonomous underwater vehicle. *Conserv. Biol.* **33**, 1174–1186 (2019).
26. Jackson-Bué, T. et al. Seabed morphology and bed shear stress predict temperate reef habitats in a high-energy marine region. *Estuar. Coast. Shelf Sci.* **274**, 107934 (2022).
27. Wright, P., Jensen, H. & Tuck, I. The influence of sediment type on the distribution of the lesser sandeel, Ammodytes marinus. *J. Sea Res.* **44**, 243–256 (2000).
28. Langton, R., Davies, I. M. & Scott, B. E. Seabird conservation and tidal stream and wave power generation: information needs for predicting and managing potential impacts. *Mar. Policy* **35**, 623–630 (2011).
29. Galparsoro, I., Borja, A. & Uyarra, M. C. Mapping ecosystem services provided by benthic habitats in the European North Atlantic Ocean. *Front. Mar. Sci.* **1**, 23 (2014).
30. Haines-Young, R. & Potschin, M. B. Common international classification of ecosystem services (cices) v5.1 and guidance on the application of the revised structure. P. 53. https://www.cices.eu (2018).
31. Bauer, J. E. et al. The changing carbon cycle of the coastal ocean. *Nature* **504**, 61–70 (2013).
32. Pauly, D. et al. Towards sustainability in world fisheries. *Nature* **418**, 689–695 (2002).
33. Amjadian, P., Neill, S. P. & Martí Barclay, V. Characterizing seabed sediments at contrasting offshore renewable energy sites. *Front. Mar. Sci.* **10**, 1156486 (2023).
34. Amoudry, L. et al. A scoping study on: research into changes in sediment dynamics linked to marine renewable energy installations. *NERC Marine Renewable Energy Theme Action Plan Report,* Vol. 102, (British Geological Survey, Edinburgh, UK, 2009).
35. van Berkel, J. et al. The effects of offshore wind farms on hydrodynamics and implications for fishes. *Oceanography* **33**, 108–117 (2020). Special issue on understanding the effects of offshore wind energy development on fisheries (December 2020).
36. Christiansen, N., Carpenter, J. R., Daewel, U., Suzuki, N. & Schrum, C. The large-scale impact of anthropogenic mixing by offshore wind turbine foundations in the shallow North Sea. *Front. Mar. Sci.* **10**, 1178330 (2023).
37. Carpenter, J. R. et al. Potential impacts of offshore wind farms on north sea stratification. *PLoS ONE* **11**, e0160830 (2016).
38. Aldridge, J. N., Parker, E. R., Bricheno, L. M., Green, S. L. & van der Molen, J. Assessment of the physical disturbance of the northern European continental shelf seabed by waves and currents. *Cont. Shelf Res.* **108**, 121–140 (2015).
39. Wilson, R. J., Speirs, D. C., Sabatino, A. & Heath, M. R. A synthetic map of the north-west European shelf sedimentary environment for applications in marine science. *Earth Syst. Sci. Data* **10**, 109–130 (2018).
40. Coughlan, M. et al. A new seabed mobility index for the Irish Sea: modelling seabed shear stress and classifying sediment

mobilisation to help predict erosion, deposition, and sediment distribution. *Cont. Shelf Res.* **229**, 104574 (2021).
41. Uehara, K., Scourse, J. D., Horsburgh, K. J., Lambeck, K. & Purcell, A. P. Tidal evolution of the northwest European shelf seas from the last glacial maximum to the present. *J. Geophys. Res. Oceans* **111,** C09025 (2006).
42. Bricheno, L. M., Wolf, J. & Aldridge, J. Distribution of natural disturbance due to wave and tidal bed currents around the UK. *Cont. Shelf Res.* **109**, 67–77 (2015).
43. Jenkins, L. J. et al. The temporal clustering of storm surge, wave height, and high sea level exceedances around the UK coastline. *Nat. Hazards* **115**, 1761–1797 (2023).
44. Birchenough, S. N. R. et al. Climate change and marine benthos: a review of existing research and future directions in the North Atlantic. *Wiley Interdiscip. Rev. Clim. Change* **6**, 203–223 (2015).
45. Bricheno, L. et al. Climate change impacts on storms and waves relevant to the UK and Ireland. *MCCIP Science Review 2025,* 24 (MCCIP Science Review, 2025). https://doi.org/10.14465/2025.reu09.str.
46. Aksenov, Y. et al. Safer operations in changing ice-covered seas: Approaches and perspectives. in *IUTAM Symposium on Physics and Mechanics of Sea Ice* Vol. 39 of *IUTAM Bookseries* (eds Tuhkuri, J. & Polojärvi, A.) https://doi.org/10.1007/978-3-030-80439-8_12 (Springer, 2022).
47. Bugnot, A. B. et al. Current and projected global extent of marine built structures. *Nat. Sustain.* **4**, 33–41 (2021).
48. Lemasson, A. J. et al. A global meta-analysis of ecological effects from offshore marine artificial structures. *Nat. Sustain.* **7**, 485–495 (2024).
49. Wakelin, S. L., Artioli, Y., Holt, J. T., Butenschön, M. & Blackford, J. Controls on near-bed oxygen concentration on the northwest European continental shelf under a potential future climate scenario. *Prog. Oceanogr.* **187**, 102400 (2020).
50. Palmer, M. et al. *UKCP18 Marine Report* Technical Report, NERC Archive, http://nora.nerc.ac.uk/id/eprint/522257/ (2018).
51. De Dominicis, M., Wolf, J. & O'Hara Murray, R. Comparative effects of climate change and tidal stream energy extraction in a shelf sea. *J. Geophys. Res. Oceans* **123**, 5041–5067 (2018).
52. Haigh, I. D. et al. The tides they are a-changin': a comprehensive review of past and future nonastronomical changes in tides, their driving mechanisms, and future implications. *Rev. Geophys.* **58**, e2018RG000636 (2020).
53. Talke, S. A. & Jay, D. A. Changing tides: the role of natural and anthropogenic factors. *Annu. Rev. Mar. Sci.* **12**, 121–151 (2020).
54. Khojasteh, D., Felder, S., Heimhuber, V. & Glamore, W. A global assessment of estuarine tidal response to sea level rise. *Sci. Total Environ.* **894**, 165011 (2023).
55. Komen, G. J. et al. *Dynamics and Modelling of Ocean Waves* Vol. 532 (Cambridge University Press, 1994).
56. Nicholls, R. J. & Cazenave, A. Sea-level rise and its impact on coastal zones. *Science* **328**, 1517–1520 (2010).
57. Haigh, I. D. et al. Timescales for detecting a significant acceleration in sea level rise. *Nat. Commun.* **5**, 4635 (2014).
58. Nerem, R. S. et al. Climate-change–driven accelerated sea-level rise detected in the altimeter era. *Proc. Natl. Acad. Sci. USA* **115**, 2022–2025 (2018).
59. Oppenheimer, M. et al. Sea level rise and implications for low-lying islands, coasts and communities. in *IPCC Special Report on the Ocean and Cryosphere in a Changing Climate* (eds Pörtner, H.-O. et al.) 321–445 (Cambridge University Press, 2019).
60. Fox-Kemper, B. et al. Ocean, cryosphere and sea level change. in *Climate Change 2021: The Physical Science Basis* (eds Masson-Delmotte, V. et al.) 1211–1362 (Cambridge University Press, 2021).
61. World Meteorological Organization. Future sea-level rise is certain, but the amount and speed are uncertain. *WMO Bull.* **74**, 2 (2025).
62. Golledge, N. R. Long-term projections of sea-level rise from ice sheets. *WIREs Clim. Change* **11**, e634 (2020).
63. Della-Marta, P. M. & Pinto, J. G. Statistical uncertainty of changes in winter storms over the North Atlantic and Europe in an ensemble of transient climate simulations. *Geophys. Res. Lett.* **36**, L14703 (2009).
64. Catto, J. L. et al. The future of midlatitude cyclones. *Curr. Clim. Change Rep.* **5**, 407–420 (2019).
65. Severino, L. G. et al. Projections and uncertainties of winter windstorm damage in Europe in a changing climate. *Nat. Hazards Earth Syst. Sci.* **24**, 1555–1578 (2024).
66. Priestley, M. D. K. & Catto, J. L. Future changes in the extratropical storm tracks and cyclone intensity, wind speed, and structure. *Wind Clim. Dyn.* **3**, 337–360 (2022).
67. IPCC. Summary for policymakers. in *Climate Change 2023: Synthesis Report. Contribution of Working Groups I, II and III to the Sixth Assessment Report of the Intergovernmental Panel on Climate Change* (eds Core Writing Team, Lee, H. & Skea, J.) 1–34. https://doi.org/10.59327/IPCC/AR6-9789291691647.001 (IPCC, 2023).
68. Wentworth, C. K. A scale of grade and class terms for clastic sediments. *J. Geol.* **30**, 377–392 (1922).
69. Unsworth, C. et al. Getting bed shear stresses right in the wake of an object in Telemac-3D 1–7. *Peer-reviewed Conference Paper, XXXth TELEMAC User Conference, Chambery, France, 8 Oct 2024* (2024).
70. Austin, M. J., Unsworth, C. A., Van Landeghem, K. J. J. & Lincoln, B. J. Enhanced bed shear stress and mixing in the tidal wake of an offshore wind turbine monopile. *Ocean Sci.* **21**, 81–91 (2025).
71. Bruns, I., Bartholomä, A., Menjua, F. & Kopf, A. Physical impact of bottom trawling on seafloor sediments in the German North Sea. *Front. Earth Sci.* **11**, 1233163 (2023).
72. O'Neill, F. G. & Summerbell, K. The mobilisation of sediment by demersal otter trawls. *Mar. Pollut. Bull.* **62**, 1088–1097 (2011).
73. Tinker, J. et al. Twenty-first century marine climate projections for the NW European shelf seas based on a perturbed parameter ensemble. *Ocean Sci.* **20**, 835–885 (2024).
74. Draper, S., Harris, J. M., Cheng, L. & White, D. J. Seabed processes: sediment transport, scour, and sedimentation. in *Encyclopedia of Maritime and Offshore Engineering* (eds Carlton, J., Jukes, P. & Choo, Y. S.) (Wiley, 2018).
75. Mellett, C. L., Carter, G. & Long, D. *Geology of the Seabed and Shallow Subsurface: The Irish Sea*. Commissioned Report CR/15/057 (British Geological Survey, 2015).
76. Spanier, R. & Kuenzer, C. Marine infrastructure detection with satellite data—a review. *Remote Sens.* **16**, 1675 (2024).
77. Gourvenec, S., Sturt, F., Reid, E. & Trigos, F. Global assessment of historical, current and forecast ocean energy infrastructure: implications for marine space planning, sustainable design and end-of-engineered-life management. *Renew. Sustain. Energy Rev.* **154**, 111794 (2022).
78. TCE. *Offshore Wind Report* Technical Report. https://www.thecrownestate.co.uk/media/4378/final-published_11720_owoperationalreport_2022_tp_250423.pdf. Accessed 3 July 2024 (The Crown Estate, 2022).
79. European Commission, Directorate-General for Energy. *Communication from the Commission to the European Parliament, the Council, the European Economic and Social Committee and the Committee of the Regions: Delivering on the EU Offshore Renewable Energy Ambitions*. Technical Report COM(2023) 668, Document 52023DC0688. https://eur-lex.europa.eu/legal-content/EN/TXT/?uri=COM:2020:741:FIN&qid=1605792629666. Accessed 3 July 2024 (European Commission, 2023).
80. Bricheno, L. M., Amies, J. D., Chowdhury, P., Woolf, D. & Timmermans, B. Climate change impacts on storms and waves relevant to the UK and Ireland. *MCCIP Sci. Rev.* **2023**, 20 (2023).

81. Mölter, T., Schindler, D., Albrecht, A. T. & Kohnle, U. Review on the projections of future storminess over the North Atlantic European region. *Atmosphere* **7**, 60 (2016).
82. Durden, J. M. et al. Perspectives in visual imaging for marine biology and ecology: from acquisition to understanding. in *Oceanography and Marine Biology: An Annual Review* Vol. 54 (eds Hughes, R. N., Hughes, D. J., Smith, I. P. & Dale, A. C.) 9–80 (Taylor & Francis, 2016).
83. Couldrey, A. J., Benson, T., Knaapen, M. A., Marten, K. V. & Whitehouse, R. J. Morphological evolution of a barchan dune migrating past an offshore wind farm foundation. *Earth Surf. Process. Landf.* **45**, 2884–2896 (2020).
84. Gates, A. R. et al. Ecological role of an offshore industry artificial structure. *Front. Mar. Sci.* **6**, 675 (2019).
85. Chambel, J. et al. A comprehensive review on scour and scour protections for complex bottom-fixed offshore and marine renewable energy foundations. *Ocean Eng.* **304**, 117829 (2024).
86. SOWEC. *Collaboration for Environmental Mitigation and Nature Inclusive Design (CEMNID)*. Technical Report, A-100906-S00-A-REPT-007 (SOWEC, 2024).
87. Robertson, M., Locke, S., Uttley, M., Helmer, L. & Kean-Hammerson, J. Exploring the role of offshore wind in restoring priority marine habitats. Report (Blue Marine Foundation, 2021).
88. Lopazanski, C. et al. Principles for climate resilience are prevalent in marine protected area management plans. *Conserv. Lett.* **16**, e12972 (2023).
89. Hoppit, G., Schmidt, D. N., Brazier, P., Mieszkowska, N. & Pieraccini, M. Are marine protected areas an adaptation measure against climate change impacts on coastal ecosystems? A UK case study. *Nat. Based Solut.* **2**, 100030 (2022).
90. Brito, J. C. & Naia, M. Coping with sea-level rise in African protected areas: priorities for action and adaptation measures. *BioScience* **70**, 924–932 (2020).
91. Keller, B. D. et al. Climate change, coral reef ecosystems, and management options for marine protected areas. *Environ. Manag.* **44**, 1069–1088 (2009).
92. Naylor, L. A. et al. Stormy geomorphology: geomorphic contributions in an age of climate extremes. *Earth Surf. Process. Landf.* **42**, 166–190 (2017).
93. Mitchell, S. Chapter 30 - sediment transport and marine protected areas. in *Marine Protected Areas* (eds Humphreys, J. & Clark, R. W.) 587–598. https://www.sciencedirect.com/science/article/pii/B9780081026984000307 (Elsevier, 2020).
94. Cheng, C. H. et al. Small-scale macrobenthic community structure along asymmetrical sand waves in an underwater seascape. *Mar. Ecol.* **42**, e12657 (2021).
95. Posey, M., Lindberg, W., Alphin, T. & Vose, F. Influence of storm disturbance on an offshore benthic community. *Bull. Mar. Sci.* **59**, 523–529 (1996).
96. Kregting, L. et al. Do changes in current flow as a result of arrays of tidal turbines have an effect on benthic communities? *PLoS ONE* **11**, e0161279 (2016).
97. Jacobs, Z. L. et al. Marine heatwaves and cold spells in the Northeast Atlantic: what should the UK be prepared for? *Front. Mar. Sci.* **11**, 1434365 (2024).
98. Bruciaferri, D. et al. The impact of ocean-wave coupling on the upper ocean circulation during storm events. *J. Geophys. Res. Oceans* **126**, e2021JC017343 (2021).
99. Valiente, N. G. et al. The impact of wave model source terms and coupling strategies to rapidly developing waves across the north-west European shelf during extreme events. *J. Mar. Sci. Eng.* **9**, 403 (2021).
100. Lewis, H. W. et al. The UKC3 regional coupled environmental prediction system. *Geosci. Model Dev.* **12**, 2357–2400 (2019).
101. Lewis, H. W. et al. Can wave coupling improve operational regional ocean forecasts for the north-west European shelf? *Ocean Sci.* **15**, 669–690 (2019).
102. Dayan, H., Le Cozannet, G., Speich, S. & Thiéblemont, R. High-end scenarios of sea-level rise for coastal risk-averse stakeholders. *Front. Mar. Sci.* **8**, https://doi.org/10.3389/fmars.2021.569992 (2021).
103. Lewis, H. W. et al. The UKC2 regional coupled environmental prediction system. *Geosci. Model Dev.* **11**, 1–42 (2018).
104. Rulent, J. et al. Comparing water level estimation in coastal and shelf seas from satellite altimetry and numerical models. *Front. Mar. Sci.* **7**, 549467 (2020).
105. Gurvan, M. et al. NEMO ocean engine. *Notes du Pôle de modélisation de l'Institut Pierre-Simon Laplace (IPSL),* **v4.0**, 27, https://doi.org/10.5281/zenodo.3878122 (2019).
106. Graham, J. A. et al. AMM15: a new high-resolution NEMO configuration for operational simulation of the European North-west Shelf. *Geosci. Model Dev.* **11**, 681–696 (2018).
107. O'Dea, E. et al. Jmmp-group/co_amm15: Co9_p2.0 (v9.2.0). Zenodo, https://doi.org/10.5281/zenodo.8171688 (2023).
108. Couvelard, X. et al. Development of a two-way-coupled ocean–wave model: assessment on a global NEMO(v3.6)–WW3(v6.02) coupled configuration. *Geosci. Model Dev.* **13**, 3067–3090 (2020).
109. Hersbach, H. et al. The ERA5 global reanalysis. *Q. J. R. Meteorol. Soc.* **146**, 1999–2049 (2020).
110. Soulsby, R. L. & Clarke, S. *Bed Shear-Stress Under Combined Waves and Currents on Smooth and Rough Beds (TR 137)* Technical Report (HR Wallingford, 2005).
111. Bourdallé-Badie, R. et al. *NEMO Ocean Engine* Technical Report (Institut Pierre-Simon Laplace (IPSL), 2018).
112. Tolman, H. L. *User Manual and System Documentation of WAVEWATCH III TM Version 3.14*. Technical Note 276(220), NOAA/NWS/NCEP/MMAB, MMAB Contribution (2009).
113. Lowe, R. J. et al. Spectral wave dissipation over a barrier reef. *J. Geophys. Res. Oceans* **110**, C04001 (2005).
114. Lowe, R. J., Falter, J. L., Monismith, S. G. & Atkinson, M. J. A numerical study of circulation in a coastal reef–lagoon system. *J. Geophys. Res. Oceans* **114**, C06022 (2009).
115. Storkey, D. et al. Forecasting the ocean state using NEMO: the new foam system. *J. Oper. Oceanogr.* **3**, 3–15 (2010).
116. Soulsby, R. L. & Whitehouse, R. J. Threshold of sediment motion in coastal environments. *Pacific Coasts and Ports' 97, Proceedings of the 13th Australasian Coastal and Ocean Engineering Conference and the 6th Australasian Port and Harbour Conference, Christchurch, New Zealand, 7–11 September 1997,* Centre for Advanced Engineering, University of Canterbury: Christchurch, New Zealand, **1**, 145–150 (1997).
117. Bricheno, L. M. & Rulent, J. Model outputs containing ocean physics projections from the north western European shelf from 1992–2093 (version 1). https://doi.org/10.5285/38626589-5885-fff9-e063-7086abc09721 (2025).
118. Bricheno, L. M. & Rulent, J. Wave projections from the north western european shelf modelled from 1992–2093. https://doi.org/10.5285/38624d82-baec-fcd8-e063-7086abc0e25c (2025).
119. Bricheno, L. M., Rulent, J., Unsworth, C. A., Van Landeghem, K. J. J. & McCarron, C. J. Model outputs containing seabed mobility projections from the north western european shelf from 1992–2093 version 2. https://www.bodc.ac.uk/data/published_data_library/catalogue/10.5285/3bc6687c-00ad-d305-e063-7086abc08650/ (2025).

Acknowledgements

This research has been supported by the NERC ECOWind-ACCELERATE project (grant no. NE/X008886/1) awarded to PI K.J.J.V.L. This work used the ARCHER2 UK National Supercomputing Service (http://www.archer2.ac.uk) and JASMIN, the UK's collaborative data analysis environment (https://

www.jasmin.ac.uk). The authors also would like to thank Viridien, especially Efrem Verderio and Federico Miorelli, for their contribution of HPC services and support for this project. The authors' work builds on the UK Regional Environmental Prediction, in collaboration between the Centre for Ecology & Hydrology (CEH), the Met Office, the National Oceanography Centre (NOC) and Plymouth Marine Laboratory (PML). The authors would like to thank the British Oceanographic Data Centre (BODC) for their assistance with publishing the underpinning datasets.

Author contributions

J.R. set up and ran the NEMO ocean numerical model on HPC, contributed to method development, analysed the data, and led the manuscript drafting. L.B. set up and ran the WaveWatchIII wave model on HPC, contributed to method development, analysed the data, supervised the numerical modelling work, and contributed to manuscript drafting. C.M.C. contributed to methods and the interpretation of sediment transport capacity, and contributed to manuscript drafting. C.U. contributed to methods and the interpretation of sediment transport capacity, provided datasets for validation, and contributed to manuscript drafting. M.J.A. contributed to results interpretation, provided datasets for validation, and contributed to manuscript drafting. R.J.S.W. contributed to methods and the interpretation of sediment transport capacity, and contributed to manuscript drafting. N.G.H. provided technical support in the development of the numerical model, assisted with preliminary modelling experiments, and contributed to manuscript drafting. D.P.G. supported the development of HPC experiments and technical development. A.W. developed modifications to the NEMO seabed stress source code routine and contributed to manuscript drafting. V.A.I.H. contributed to results interpretation and manuscript drafting. K.J.J.V.L. secured funding, contributed to method development, assisted with data interpretation, and contributed to manuscript drafting.

Competing interests

The authors declare no competing interests.

Additional information

Supplementary information The online version contains supplementary material available at https://doi.org/10.1038/s43247-026-03500-4.

Correspondence and requests for materials should be addressed to Julia Rulent.

Peer review information *Communications Earth & Environment* thanks Rae Taylor-Burns, Jian Su and the other, anonymous, reviewer(s) for their contribution to the peer review of this work. Primary Handling Editors: Shan Liu and Alice Drinkwater. A peer review file is available

Reprints and permissions information is available at http://www.nature.com/reprints

Publisher's note Springer Nature remains neutral with regard to jurisdictional claims in published maps and institutional affiliations.